Nano Energy 57 (2019) 432–439

Contents lists available at ScienceDirect

Nano Energy

journal homepage: www.elsevier.com/locate/nanoen

Full paper

Largely enhanced triboelectric nanogenerator for efficient harvesting of water wave energy by soft contacted structure

Ping Cheng[a,b,c,1], Hengyu Guo[a,c,d,1], Zhen Wen[b,1], Chunlei Zhang[a,c], Xing Yin[a,c], Xinyuan Li[a,c], Di Liu[a,c], Weixing Song[a], Xuhui Sun[b], Jie Wang[a,c,*], Zhong Lin Wang[a,c,d,*]

[a] Beijing Institute of Nanoenergy and Nanosystems, Chinese Academy of Sciences, Beijing 100083, China
[b] Institute of Functional Nano and Soft Materials (FUNSOM), Jiangsu Key Laboratory for Carbon-Based Functional Materials and Devices, and Joint International Research Laboratory of Carbon-Based Functional Materials and Devices, Soochow University, Suzhou 215123, China
[c] College of Nanoscience and Technology, University of Chinese Academy of Sciences, Beijing 100049, China
[d] School of Materials Science and Engineering, Georgia Institute of Technology, Atlanta, GA 30332, USA

ARTICLE INFO

Keywords:
Triboelectric nanogenerator
Silicone rubber
Water wave energy harvesting
Soft contact

ABSTRACT

Triboelectric nanogenerator (TENG) is a new emerging and cost-effective technology for harvesting water wave energy because of its unmatchable performance in low frequency and randomly directed motions. Here, we report an approach that significantly increased the output power of spherical TENGs by optimizing both materials and structural design. Fabricated with an acrylic hollow sphere as its shell and a rolling flexible liquid/silicone as the soft core, the soft-contact spherical triboelectric nanogenerator (SS-TENG) presents up to 10-fold enhancement to the maximum output charge compared to that of a conventional Polytetrafluoroethylene (PTFE) based hard-contact one, which is resulted from the significantly increased contact area. Besides, the output is tunable through controlling the softness of the liquid/silicone core. Our finding provides a new optimization methodology for TENGs and enable its more promising usage in harvesting large-scale blue energy from water wave in oceans as well as feeble but ubiquitous wind energy.

1. . Introduction

With the rapid development of economics and the fast growing demand of energy, clean and renewable energy has been of much significance and urgency [1–3]. Oceans cover over 70% of earth's surface [4], which contain various kinds of clean energy such as the water wave energy, tidal energy and ultrasonic energy [5,6]. Nonetheless, most of the ocean energy is hard to harvest for technical reasons. Conventional approaches harvesting water wave energy to generate the electricity are based on bulky and heavy electromagnetic generator (EMG) which is not convenient to be installed in ocean and hard to be driven. Triboelectric nanogenerator, based on coupling of triboelectrification effect and electrostatic induction [7], shows good performance in power generation [8–12] or ambient mechanical energy harvesting [13–15]. They also have merits of light weight, simple structure, low cost and abundant choice of materials [16–19]. Our previous work indicated that the TENG has a much better performance than that of the EMG at low frequency (typically 0.1–3 Hz) [20]. Meanwhile, the frequency of water wave in the ocean is generally below 2 Hz. Therefore, the TENG has been demonstrated to effectively harvest water wave energy [21,22]. The spherical TENG networks have been demonstrated to be an effective approach toward massive harvesting of water wave energy in ocean. The first spherical TENG was proposed in 2014 in single electrode mode with many small polyfluoroalkoxy (PFA) balls as the triboelectric material, whose output power is 128 μW [23] and was soon improved to 0.5 mW (transferred charge as 1.2 nC) by a fully enclosed cylindrical TENG [24]. Polytetrafluoroethylene (PTFE), another triboelectric material, was adopted by spherical TENGs in both contact-separate mode [25] and freestanding mode which enhanced the transferred charge to 20 nC [26]. Recently, a spherical TENG using modified silicone rubber as the triboelectric material boosted the transferred charge to 60 nC at a frequency of 3 Hz [27].

The output power density of TENG is proportional to the square of its triboelectric surface charge density due to the open-circuit voltage and short-circuit current are proportional to it simultaneously [28,29]. Therefore, the triboelectric charge density is the figure-of-merits to evaluate the performance of TENG [30], which is largely determined by the effectiveness of contact between two triboelectric surfaces [31].

* Corresponding authors at: Beijing Institute of Nanoenergy and Nanosystems, Chinese Academy of Sciences, Beijing 100083, China.
E-mail addresses: wangjie@binn.cas.cn (J. Wang), zhong.wang@mse.gatech.edu (Z.L. Wang).
[1] P. Cheng, H. Guo and Z. Wen contributed equally to this work.

https://doi.org/10.1016/j.nanoen.2018.12.054
Received 21 November 2018; Received in revised form 11 December 2018; Accepted 17 December 2018
Available online 20 December 2018
2211-2855/

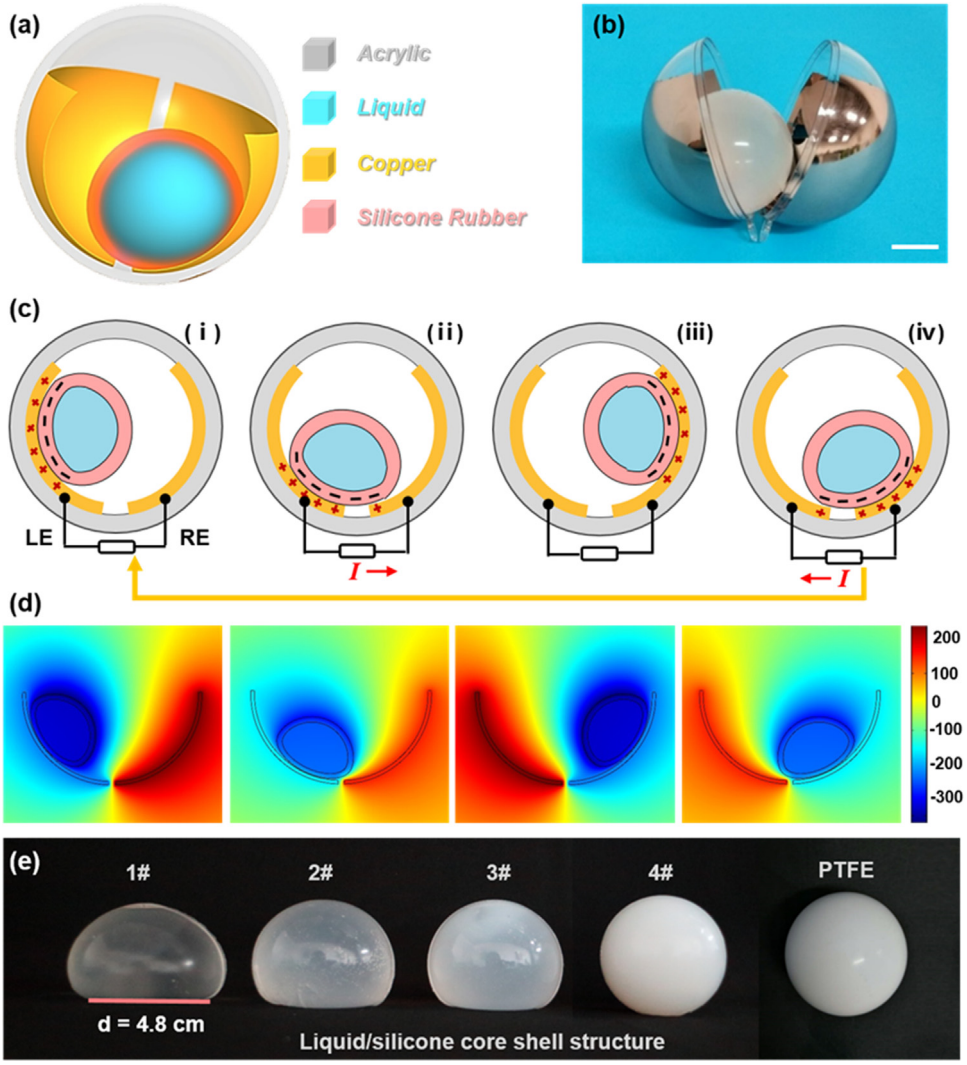

Fig. 1. Schematic illustration and working mechanism of the soft-contact model spherical triboelectric nanogenerator (SS-TENG). (a) Structural scheme of the soft-contact model spherical TENG (SS-TENG) with a flexible rolling sphere. (b) Photograph of a SS-TENG (scale bar, 1.5 cm). (c) Charge distributions scheme of the device under short circuit condition and (d) the corresponding simulated potential distributions under open circuit condition respectively. (e) Photographs of the flexible rolling sphere (1# to 4#) with different shell parameters compared to rigid PTFE sphere.

Hence, the hard contact between core and shell in spherical TENG weakens its power outputs. To solve this issue, we design a novel soft-contact spherical TENG that replaces the hard triboelectric material (such as PTFE) by a soft core made with liquid/silicone, which largely increases the contact area so as to generate much more triboelectric charges, where the effective contact area can be tuned by the thickness of the silicone shell. Besides flexibility, silicone rubber also presents a stronger tendency to gain electrons than PTFE in triboelectric series, which amplifies charge density in each single contact. Compared to the benchmark charge density of PTFE based spherical TENG, it is demonstrated that the optimized soft-contact model spherical TENG (SS-TENG) can deliver 2 times enhancement at a low frequency of ~2 Hz, and up to10-fold enhancement at 5 Hz.

2. Results

2.1. Structure and working mechanism of SS-TENG

The novel structure of the SS-TENG for harvesting water wave energy is schematically illustrated in Fig. 1**a**, which mainly consists of a hollow acrylic sphere outside, two copper electrodes and a rolling soft liquid/silicone core of different thicknesses inside. Fig. 1**b** shows an image of the fabricated device. When driven by water waves, the soft rolling sphere will move back and forth between two electrodes, providing alternating current to an external load. To increase the contact area so as to enhance the electric outputs of the TENG, silicone rubber was chosen as the material of triboelectric material shaped in a hollow sphere with some water inside, which ensures adequate inertia to make full contact when motion direction is altered. Photographs of the device without copper electrodes are displayed in Fig. S1. The diameter of outside shell sphere is 7 cm and that of the silicone rubber sphere is 5 cm. As illustrated in Fig. 1**c,** its working principle is based on the triboelectrification effect [2]. The dielectric silicone rubber and the electrodes are uncharged at the first, static charges are then introduced by triboelectrification effect when they physically contact. Specifically, when the silicone rubber sphere slides against the Cu electrodes with surfaces in contact, the triboelectric effect will render silicone rubber surface with negative charges, and Cu electrodes with positive charges (Fig. 1**c** < **i** >). Then, when the silicone rubber slides towards the right-hand electrode (RE), the positive charges in the loop will flow from the LE to the RE via the load to screen the local field of the non-mobile negative charges on the dielectric (Fig. 1**c** < **ii** >). When the silicone rubber reaches the overlapping position of the RE, all of the positive charges will then be driven to the RE (Fig. 1**c** < **iii** >).

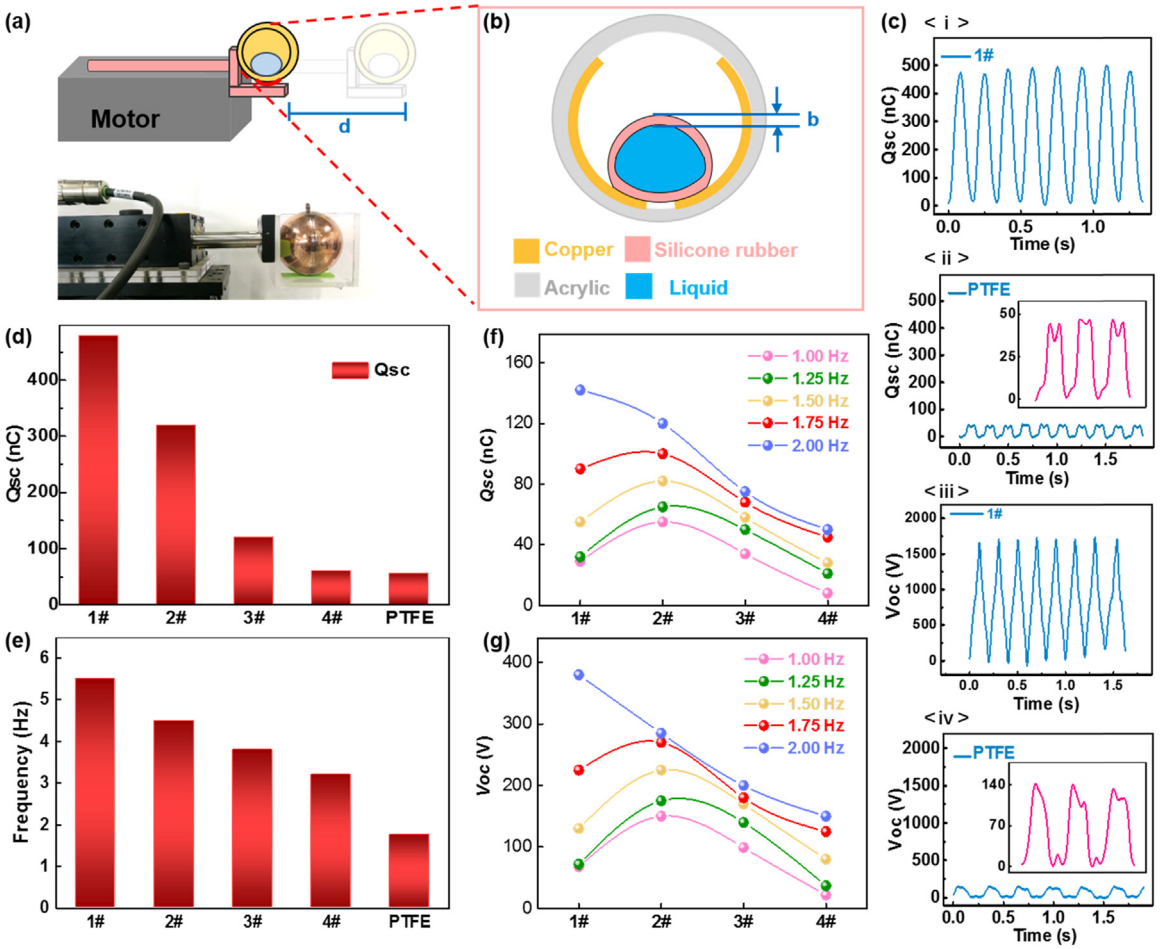

Fig. 2. Electrical output performance characterization of SS-TENGs. (a) Experimental setup for quantitative investigation SS-TENG individually. (b) The zoom-in illustration reveals thickness of the silicone shell would affect the flexibility of the rolling sphere. (c) The maximum transferred charge (Q_{sc}) and open-circuit voltage (V_{oc}) curves of the SS-TENG-1 and S-TENG respectively. The insets show enlarged views. (d) The maximum transferred charge of SS-TENGs. (e) Frequency to reach the maximum transferred charge. (f) Transferred charge of SS-TENGs at different frequencies (displacement, 50 mm). (g) Open-circuit voltage of SS-TENGs at different frequencies (displacement, 50 mm).

Subsequently, a backward sliding of the silicone rubber from the RE to the LE should drive the flow of the positive charges in the same direction, forming a reverse current in the load (Fig. 1**c** < **iv** >) [29]. The simulation results of potential distribution by COMSOL are presented in Fig. 1**e,** which show different states of the silicone rubber core respectively. In order to study the effect of different softness on the output, several spheres with different softness of silicone are fabricated, numbered from 1# to 4#, and tested the diameter of contact area (Dca) to represent the softness, which is 4.8 cm, 3.9 cm, 3.0 cm and 0.4 cm, respectively. A PTFE hard sphere is also presented in Fig. 1**e**, which can only make point contact.

2.2. Optimization of output performance

Fig. 2 presents the electrical characterizations of SS-TENGs working at different frequency. The illustration and the photograph of the experimental setup are shown in Fig. 2(**a**). Liner motor was utilized to provide the impact agitation. The displacement was defined as *d* that has been made a sign on the sketch map (Supplementary Note 2). Fig. 2**b** illustrates enlarged details of the SS-TENG unit. With the decreasing of the inner flexible silicone sphere's thickness named *b*, the output performances improve dramatically (Fig. S2). The outputs of SS-TENG is also 10-foldly improved compared with those of the conventional spherical triboelectric nanogenerator (S-TENG) (Fig. 2**c**). The maximum transferred charge and open-circuit voltage of SS-TENG-1 can reach around 500 nC and 1600 V at proper frequency, while that of S-TENG is 50 nC. With the decrease of the silicone thickness, the maximum outputs improve rapidly, as presented in the Fig. 2(**d**) and (**e**), suggesting that the output of SS-TENG can be tuned by the thickness of soft sphere. The tunable softness ensures SS-TENG can efficiently work with various frequency of impact force, where the proper match of them releases the highest power output compared with unmatched SS-TENG. With a fixed frequency but different moving displacements (standing for different impact force), the outputs of the transferred charge, open-circuit voltage and short-circuit current are shown in the Fig. S3(**a–c**). Considering a single SS-TENG, Q_{sc}, V_{oc} and I_{sc} all improved with the increasing displacement at the same frequency of 2 Hz. SS-TENG-4, close to point-contact, has the relatively lower outputs on account of the smaller contact area. Its transferred charge is 10 nC at the displacement of 10 mm and reaches 60 nC at the displacement of 50 mm. As the thickness becoming thinner, the output performance of SS-TENG increased evidently at the same moving displacement and SS-TENG-1 keeps the best properties all the time. Its transferred charge and open-circuit voltage can reach 30 nC and 140 V respectively at the displacement of 10 mm, achieve 140 nC, 380 V when it is 50 mm. Therefore, it is quite beneficial to improve the outputs by increasing the movement displacement. In addition, the output performances of different silicone rubber spheres of different thickness at different frequency are shown in the Fig. 2(**f–g**) and Fig. S4. SS-TENG-1 shows the great properties in all tests at a frequency of 2 Hz on account

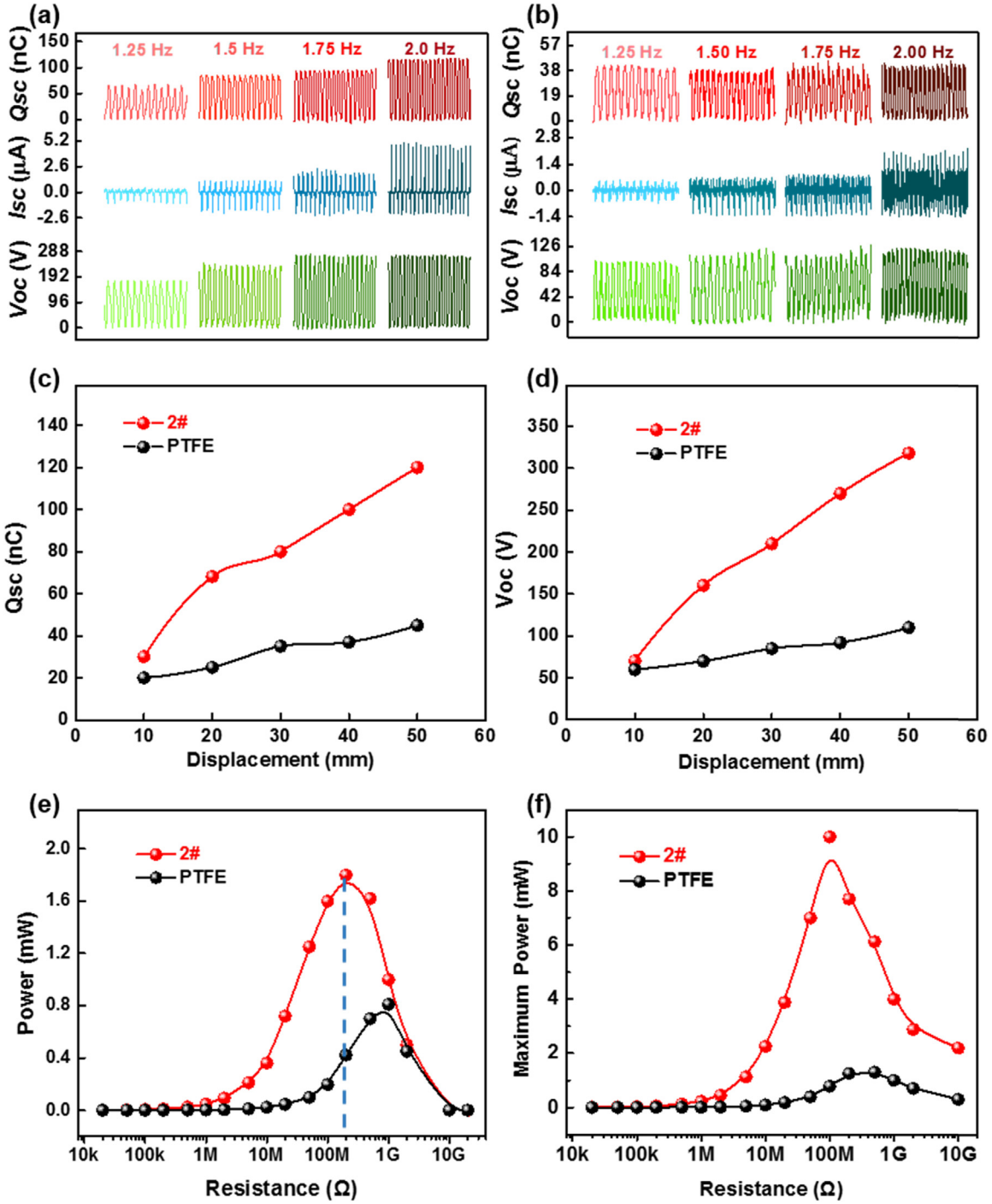

Fig. 3. The electrical output comparisons between SS-TENG and S-TENG. Typical electric output curves of SS-TENG-2 (a) and S-TENG (b) under various working frequencies. (c) The measured transferred charge (Q_{sc}), (d) open-circuit voltage of SS-TENG-2 and S-TENG at different displacements. The output power comparison of SS-TENG-2 and S-TENG at 2 Hz (e) and at 5 Hz (f).

of larger contact area. With the frequency decreasing, open-circuit voltage and transferred charge of SS-TENG-2 reveal an optimum output performance, for lower friction force compared with SS-TENG-1 and larger contact area compared with SS-TENG-3, 4. Therefore, SS-TENG-2 is a better choice to harvest the low frequency (< 2 Hz) water wave energy compared with the others. Meanwhile, output performances of the SS-TENG are also affected by size of the silicone rubber sphere and the volume of water in silicone rubber sphere (Fig. S5). As the size of silicone rubber sphere becomes larger, the outputs of SS-TENG increase accordingly. Therefore, the output can be improved by increasing the size of the silicone rubber sphere. In the Fig. S6, the outputs of SS-TENG increases obviously with water volume increasing, for the water increases the gravity and inertia of the silicone rubber ball to achieve a better state of motion.

2.3. Comparisons of SS-TENG and S-TENG

The detail of the output performances of SS-TENG-2 and S-TENG are shown in Fig. 3(**a**) and (**b**). The results were tested by a linear motor under various frequencies, and the displacement of a movement is 50 mm. When the frequency increases from 1.25 Hz to 2 Hz, the transferred charge and open-circuit voltage of SS-TENG improve

obviously, reaching 110 nC and 280 V, respectively, for the increased deformation of the silicone rubber sphere can improve the contact area. Meanwhile, short-circuit current exhibits a clear increasing trend from 1 μA to 5 μA with the increase of frequency. However, compared with the SS-TENG, the transferred charge and open-circuit voltage of S-TENG almost remains stably, and they are maintained at a relatively lower value of 45 nC and 130 V, respectively. The short-circuit current has a little improvement with the increasing frequency, but it increases slowly, which only reaches 1.8 μA at a frequency of 2 Hz. These two figures indicate that the hard point-contact S-TENG extremely limits the improvement of the outputs. Under the frequency of 2 Hz, the output comparisons between SS-TENG-2 and S-TENG at various displacement are shown in Fig. 3(**c–e**) and Fig. S7. The transferred charge of S-TENG is 20 nC at a displacement of 10 mm, which agrees with the reported value [26]. It improves with the increasing of the displacement and reaches 50 nC at 50 mm. The value of SS-TENG-2 not only is slightly higher than that of S-TENG at a displacement of 10 mm, but also increases more rapidly with the increasing of the displacement, up to 125 nC at the displacement of 50 mm, given a more 2 times enhancement. As for open-circuit voltage (V_{oc}) and short-circuit current (I_{sc}), there are similar trends. Those of S-TENG are 100 V and 1.8 μA, and those of SS-TENG can reach 350 V and 5 μA at a displacement of 50 mm, respectively. The maximum output peak power of S-TENG at 2 Hz is 0.8 mW at the external load of 700 MΩ. The one of SS-TENG-2 reaches 1.8 mW at the external load of 200 MΩ. At the same external load 200 MΩ, the output peak power of S-TENG is only 0.4 mW, which indicates there is more than 4 times enhancement for SS-TENG. As we known, the output power will increase with the increasing frequency. The maximum output peak power of S-TENG reaches 1.2 mW at a frequency of 5 Hz, and the value of SS-TENG-2 achieves 10 mW, given a 8-times enhancement (Fig. 3**f**). All of these results indicate that soft silicone rubber sphere as the triboelectric material is a better choice for harvesting water wave energy.

2.4. Applications of SS-TENG in wearable electronics

To explore the stability of the fabricated device, 70,000 test cycles have been carried out by using a linear motor. The outputs of the transferred charges (Q_{sc}), open-circuit voltage (V_{oc}) and the short-circuit current (I_{sc}) remain almost stable (Fig. 4**a**). The details are presented in Fig. S8. A self-powered system was built to demonstrate the SS-TENG efficiently harvesting water wave energy to drive electronics. Fig. 4**b** presents the circuit diagram of the self-powered system, where the capacitor and the SS-TENG are connected by a full-wave rectifier. The voltage of the capacitor is monitored by a voltmeter. The first phase is the charging process when switch K1 is on, switch K2 is off and the capacitor is charged by the TENGs. As shown in Fig. 4**c**, the voltages of the same capacitor (2.2 μF) are charged to 4.5 V by S-TENG and 6 V by SS-TENG-2 in 30 s at 2.0 Hz. Furthermore, SS-TENG-1 can charge the capacitor to 8 V in 30 s. The equivalent galvanostatic current (I_{eg}) of S-TENG, SS-TENG-2 and SS-TENG-1 can be calculated as 0.33 μA, 0.44 μA and 0.55 μA respectively (Supplementary Note 9). Although, the outputs of SS-TENG unit is not high enough, the power module circuit and energy storage device are significant for TENG to efficiently utilize the electricity [32–34]. Also, a mass of SS-TENG units can be connected in parallel to achieve a higher output. By SS-TENG-2, the voltages of capacitors with a capacitance of 2.2 μF, 4.5μF and 10 μF can be charged to 6 V, 3 V and 1.8 V in 30 s, respectively (Fig. 4**d**). The accumulated charge is 4.5 μC by SS-TENG-2 at 1 Hz. Along with the increase of the frequency, the accumulated charge improves and achieves 20 μC at 2 Hz (Fig. 4**e**). After that, SS-TENG was utilized to charge the capacitor and power a watch while switch K1 is on and switch K2 is off. When the voltage reach around 1.2 V, the switch K2 is on and the SS-TENG can be a self-power source to drive the watch (Fig. 4**f**). The inset is a photography of a watch driven by SS-TENG-2.

2.5. Output performance of SS-TENG in water

In order to analyze their output performances to harvesting water wave energy, SS-TENG and S-TENG are tested in the wave tank with

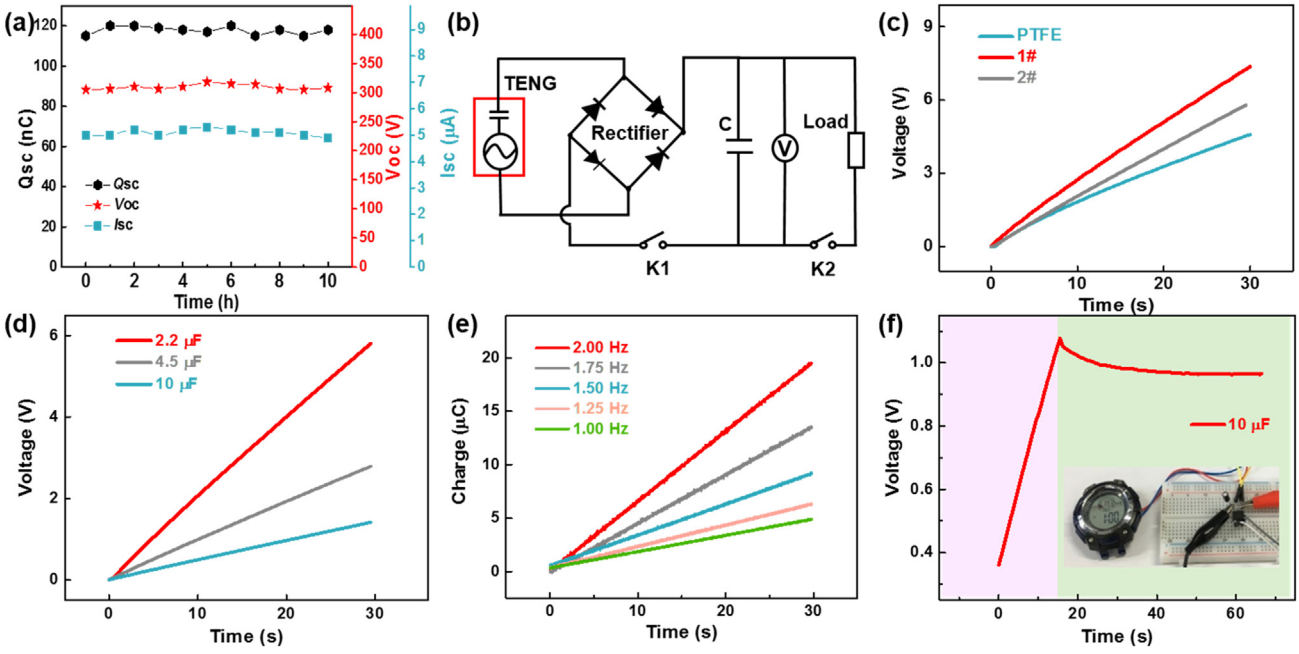

Fig. 4. Applications of SS-TENGs for harvesting water wave energy. (a) Long-term stability test of a SS-TENG that lasts for 70,000 cycles (2#, 2.0 Hz). (b) Circuit diagram of the self-powered system consisting of a TENG and a capacitor. (c) The charging curves of different SS-TENGs and S-TENG at 2.0 Hz for a capacitor (2.2 μF). (d) The charging curves of SS-TENG-2 at 2.0 Hz for different capacitors (2.2 μF, 1.5 μF, 10 μF). (e) The charging curves of SS-TENG-2 at different frequency for capacitor (2.2 μF). (f) Charging curve of the capacitor (10 μF) when an electronic watch is driven by the SS-TENG simultaneously. The inset is a photography of a watch driven by SS-TENG-2.

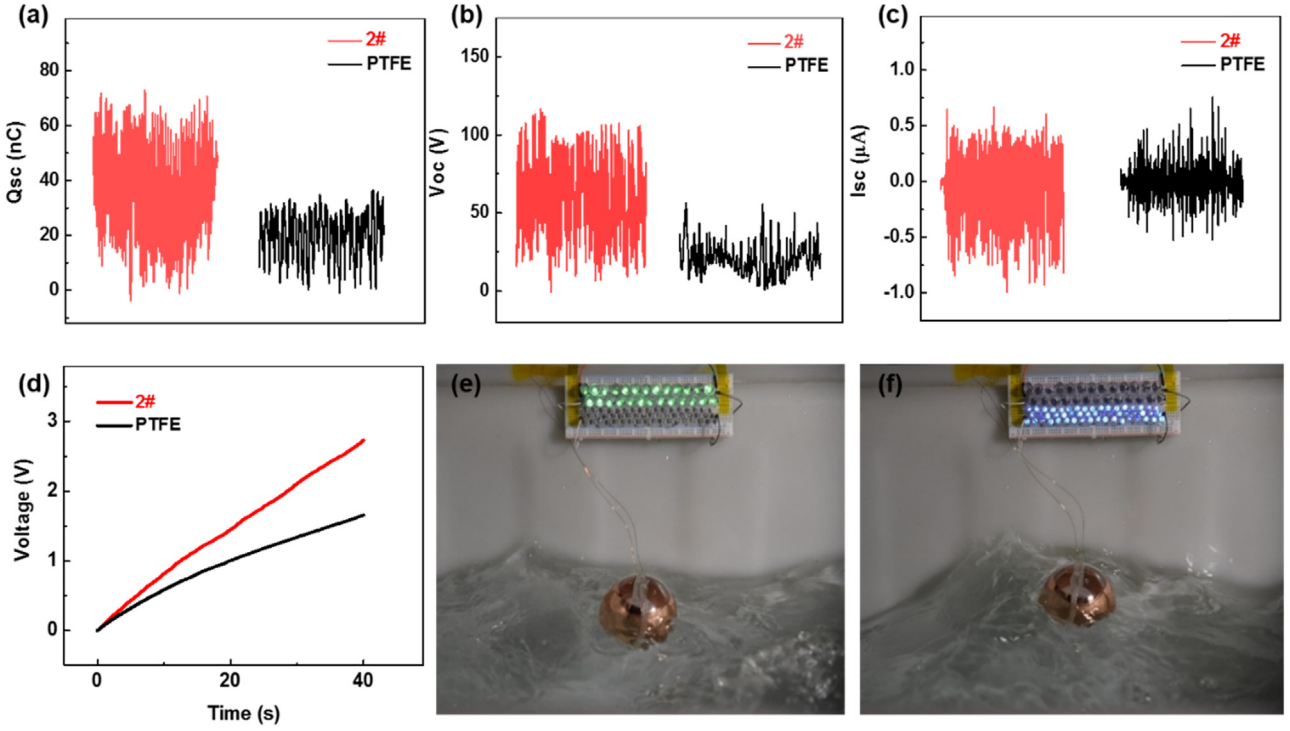

Fig. 5. Output comparisons of the SS-TENG with S-TENG in water. (a) The transferred charge (Q_{sc}), (b) open-circuit voltage (V_{oc}) and (c) short circuit current (I_{sc}) curves of the SS-TENG-2 and S-TENG at the frequency of 2 Hz, respectively. (d) The charging curves of SS-TENG and S-TENG for a capacitor (2.2 μF) at the frequency of 2 Hz. (e–f) Demonstrations of the SS-TENG-2 as a power source to light the LEDs.

simulated water waves. The output comparisons between SS-TENG-2 and S-TENG at a frequency of 2 Hz are shown in Fig. 5(**a–c**). The transferred charge of S-TENG is 30 nC and that of SS-TENG-2 can reach 65 nC; The open circuit voltage of S-TENG is 40 V and that of SS-TENG-2 reaches 90 V. Meanwhile, the short-circuit current of S-TENG and SS-TENG-2 can reach 0.4 μA and 0.8 μA, respectively. All of these values have a decrease compared with those in air. But the SS-TENG-2 still presents a better performance than that of S-TENG. Voltages of capacitor with a capacitance of 2.2 μF can be charged to around 3 V by SS-TENG-2 and 1.6 V by S-TENG in 40 s at a frequency of 2 Hz (Fig. 5**d**). All of these results indicate that the outputs of SS-TENG improve obviously compared with the S-TENG. Fig. 5(**e–f**) and Movie S1 are photographs and movie of SS-TENG-2 as a power source working in water lighting 26 green LEDs (rated power, 45 mW) or 56 blue LEDs (rated power, 45 mW) by harvesting the water wave energy. Because triboelectric nanogenerator converts frictional energy into electricity by producing alternating current, the LEDs will be lit alternately, which circuit diagram is shown in Fig. S9.

Supplementary material related to this article can be found online at doi:10.1016/j.nanoen.2018.12.054.

3. Discussion

In conclusion, we present a soft-contact spherical triboelectric nanogenerator (SS-TENG) to harvest water wave energy for the first time, which largely increases the contact area and greatly improves output performance. Its maximum transferred charge (Q_{sc}) can reach around 500 nC, exceeding that of a conventional hard-contact TENG-PTFE up to 10 times. Furthermore, its structure parameter can be turned to match the outside impact frequency, which is a practical and solid progress of TENG for harvesting low-frequency energy containing in many forms in nature, from fierce water wave in ocean to feeble and ubiquitous wind in air.

4. Methods

4.1. Fabrication of the SS-TENG

Two copper films (100 nm in thickness) were deposited by magnetron sputtering(Discovery635) for electrodes which stick to acrylic hollow sphere (d = 7 cm) inner surface. Two lead wires were connected respectively to the two sets of electrodes. The liquid silicone rubber was obtained by mixing the silicone base and curing it with a volume ratio of 1:1 (Exoflex supersoft silicone 0050 manufactured by Smooth-On, Inc.) in a beaker. Next, we smeared the mixture over the inner surface of another acrylic sphere (d = 5 cm, with the releasing agent poured on the surface in advance) at 30 °C for 6 h until the silicone was cured. Finally, we took it from the sphere and the soft sphere can be obtained. Finally, we injected some water into the hollow sphere and smeared a little mixed silicone rubber on the hole for 44 h until the silicone was cured.

4.2. Electrical measurement of the TENGs

For the electric output measurement of the TENG, a linear motor (TSMV120-1S) was applied to drive the SS-TENG. Two propeller pumps (RW-20) were used to simulate the water wave. The programmable electrometer (Keithley model 6514) was adopted to test the short-circuit current and transferred charge and a mixed domain oscilloscope (MDO3024) was used to test the open-circuit voltage. A potentiostat (Biologic, VMP3) was utilized to test the voltage of the capacitor in the self-charging power system.

Acknowledgement

Research was supported by the National Key R & D Project from Minister of Science and Technology (2016YFA0202704), Beijing Municipal Science and Technology Commission (Z171100000317001, Z171100002017017, Y3993113DF), National Natural Science

Foundation of China (Grant No. 61774016, 21773009, 51432005, 5151101243, 51561145021) Patents have been filed based on the research results presented in this manuscript.

Author contributions

P.C., H.G., Z.W. J.W. and Z.L.W. conceived the idea, analysed the data and wrote the paper. P.C. and H.G. designed the materials of the triboelectric nanogenerators. P.C., Z.W and J.W. optimized the structure of the triboelectric nanogenerators. C.Z., X.S. and W.S. derived the theories for structure optimization. X.L., X.Y. and D.L. helped with the experiments. All the authors discussed the results and commented on the manuscript.

Competing interests

The authors declare no competing financial interest.

Appendix A. Supporting information

Supplementary data associated with this article can be found in the online version at doi:10.1016/j.nanoen.2018.12.054.

References

[1] D. Gielen, F. Boshell, D. Saygin, Climate and energy challenges for materials science, Nat. Mater. 15 (2) (2016) 117–120.
[2] F.R. Fan, Z.Q. Tian, Z.L. Wang, Flexible triboelectric generator!, Nano Energy 1 (2) (2012) 328–334.
[3] Q. Schiermeier, J. Tollefson, T. Scully, A. Witze, O. Morton, Electricity without carbon, Nature 454 (7206) (2008) 816–823.
[4] Z.L. Wang, New wave power, Nature 542 (7640) (2017) 159–160.
[5] A. Cho, To catch a wave, Science 347 (6226) (2015) (1084-1084).
[6] Y. Xi, J. Wang, Y.L. Zi, X.G. Li, C.B. Han, X. Cao, C.G. Hu, Z.L. Wang, High efficient harvesting of underwater ultrasonic wave energy by triboelectric nanogenerator, Nano Energy 38 (2017) 101–108.
[7] Z.L. Wang, On Maxwell's displacement current for energy and sensors: the origin of nanogenerators, Mater. Today 20 (2) (2017) 74–82.
[8] S.Y. Gao, J.Z. Su, X.J. Wei, M. Wang, M. Tian, T. Jiang, Z.L. Wang, Self-powered electrochemical oxidation of 4-aminoazobenzene driven by a triboelectric nanogenerator, ACS Nano 11 (1) (2017) 770–778.
[9] S.Y. Gao, Y. Chen, J.Z. Su, M. Wang, X.J. Wei, T. Jiang, Z.L. Wang, Triboelectric nanogenerator powered electrochemical degradation of organic pollutant using Pt-free carbon materials, ACS Nano 11 (4) (2017) 3965–3972.
[10] S.Y. Gao, M. Wang, Y. Chen, M. Tian, Y.Z. Zhu, X.J. Wei, T. Jiang, An advanced electro-Fenton degradation system with triboelectric nanogenerator as electric supply and biomass-derived carbon materials as cathode catalyst, Nano Energy 45 (2018) 21–27.
[11] J. Wang, Z. Wen, Y.L. Zi, P.F. Zhou, J. Lin, H.Y. Guo, Y.L. Xu, Z.L. Wang, All-plastic-materials based self-charging power system composed of triboelectric nanogenerators and supercapacitors, Adv. Funct. Mater. 26 (7) (2016) 1070–1076.
[12] J. Wang, Z. Wen, Y.L. Zi, L. Lin, C.S. Wu, H.Y. Guo, Y. Xi, Y.L. Xu, Z.L. Wang, Self-powered electrochemical synthesis of polypyrrole from the pulsed output of a triboelectric nanogenerator as a sustainable energy system, Adv. Funct. Mater. 26 (20) (2016) 3542–3548.
[13] J. Wang, X.H. Li, Y.L. Zi, S.H. Wang, Z.L. Li, L. Zheng, F. Yi, S.M. Li, Z.L. Wang, A flexible fiber-based supercapacitor-triboelectric-nanogenerator power system for wearable electronics, Adv. Mater. 27 (33) (2015) 4830–4836.
[14] X.J. Pu, H.Y. Guo, J. Chen, X. Wang, Y. Xi, C.G. Hu, Z.L. Wang, Eye motion triggered self-powered mechnosensational communication system using triboelectric nanogenerator, Sci. Adv. 3 (7) (2017).
[15] J. Wang, C.S. Wu, Y.J. Dai, Z.H. Zhao, A. Wang, T.J. Zhang, Z.L. Wang, Achieving ultrahigh triboelectric charge density for efficient energy harvesting, Nat. Commun. 8 (2017) 88.
[16] Z.L. Wang, Triboelectric nanogenerators as new energy technology and self-powered sensors - principles, problems and perspectives, Faraday Discuss. 176 (2014) 447–458.
[17] G. Zhu, B. Peng, J. Chen, Q.S. Jing, Z.L. Wang, Triboelectric nanogenerators as a new energy technology: from fundamentals, devices, to applications, Nano Energy 14 (2015) 126–138.
[18] Y. Fu, M. Zhang, Y. Dai, H. Zeng, C. Sun, Y. Han, L. Xing, S. Wang, X. Xue, Y. Zhan, Y. Zhang, A self-powered brain multi-perception receptor for sensory-substitution application, Nano Energy 44 (2018) 43–52.
[19] Y. Dai, Y. Fu, H. Zeng, L. Xing, Y. Zhang, Y. Zhan, X. Xue, A self-powered brain-linked vision electronic-skin based on triboelectric-photodetecing pixel-addressable matrix for visual-image recognition and behavior intervention, Adv. Funct. Mater. 28 (20) (2018) 1800275.
[20] Y.L. Zi, H.Y. Guo, Z. Wen, M.H. Yeh, C.G. Hu, Z.L. Wang, Harvesting low-frequency (< 5 Hz) irregular mechanical energy: a possible killer application of triboelectric nanogenerator, ACS Nano 10 (4) (2016) 4797–4805.
[21] L. Xu, Y.K. Pang, C. Zhang, T. Jiang, X.Y. Chen, J.J. Luo, W. Tang, X. Cao, Z.L. Wang, Integrated triboelectric nanogenerator array based on air-driven membrane structures for water wave energy harvesting, Nano Energy 31 (2017) 351–358.
[22] T. Jiang, Y.Y. Yao, L. Xu, L.M. Zhang, T.X. Xiao, Z.L. Wang, Spring-assisted triboelectric nanogenerator for efficiently harvesting water wave energy, Nano Energy 31 (2017) 560–567.
[23] H.L. Zhang, Y. Yang, Y.J. Su, J. Chen, K. Adams, S. Lee, C.G. Hu, Z.L. Wang, Triboelectric nanogenerator for harvesting vibration energy in full space and as self-powered acceleration sensor, Adv. Funct. Mater. 24 (10) (2014) 1401–1407.
[24] Y.J. Su, Y. Yang, X.D. Zhong, H.L. Zhang, Z.M. Wu, Y.D. Jiang, Z.L. Wang, Fully enclosed cylindrical single-electrode-based triboelectric nanogenerator, ACS Appl. Mater. Interfaces 6 (1) (2014) 553–559.
[25] Y. Yang, H.L. Zhang, R.Y. Liu, X.N. Wen, T.C. Hou, Z.L. Wang, Fully enclosed triboelectric nanogenerators for applications in water and harsh environments, Adv. Energy Mater. 3 (12) (2013) 1563–1568.
[26] X.F. Wang, S.M. Niu, Y.J. Yin, F. Yi, Z. You, Z.L. Wang, Triboelectric nanogenerator based on fully enclosed rolling spherical structure for harvesting low-frequency water wave energy, Adv. Energy Mater. 5 (24) (2015) 1501467.
[27] L. Xu, T. Jiang, P. Lin, J.J. Shao, C. He, W. Zhong, X.Y. Chen, Z.L. Wang, Coupled triboelectric nanogenerator networks for efficient water wave energy harvesting, ACS Nano 12 (2) (2018) 1849–1858.
[28] Y.L. Zi, C.S. Wu, W.B. Ding, Z.L. Wang, Maximized effective energy output of contact-separation triggered triboelectric nanogenerators as limited by air breakdown, Adv. Funct. Mater. 27 (24) (2017) 1700049.
[29] S.H. Wang, Y.N. Xie, S.M. Niu, L. Lin, Z.L. Wang, Freestanding triboelectric-layer-based nanogenerators for harvesting energy from a moving object or human motion in contact and non-contact modes, Adv. Mater. 26 (18) (2014) 2818–2824.
[30] Y.L. Zi, S.M. Niu, J. Wang, Z. Wen, W. Tang, Z.L. Wang, Standards and figure-of-merits for quantifying the performance of triboelectric nanogenerators, Nat. Commun. 6 (2015) 8376.
[31] J. Wang, S.M. Li, F. Yi, Y.L. Zi, J. Lin, X.F. Wang, Y.L. Xu, Z.L. Wang, Sustainably powering wearable electronics solely by biomechanical energy, Nat. Commun. 7 (2016) 12744.
[32] J. Kim, J. Lee, J. You, M.S. Park, M.S. Al Hossain, Y. Yamauchi, J.H. Kim, Conductive polymers for next-generation energy storage systems: recent progress and new functions, Mater. Horiz. 3 (6) (2016) 517–535.
[33] C. Vankecke, L. Assouere, A.Q. Wang, P. Durand-Estebe, F. Caignet, J.M. Dilhac, M. Bafleur, Multisource and battery-free energy harvesting architecture for aeronautics applications, Ieee Trans. Power Electr. 30 (6) (2015) 3215–3227.
[34] J. Kim, J.H. Lee, J. Lee, Y. Yamauchi, C.H. Choi, J.H. Kim, Research update: hybrid energy devices combining nanogenerators and energy storage systems for self-charging capability, Apl Mater. 5 (7) (2017).

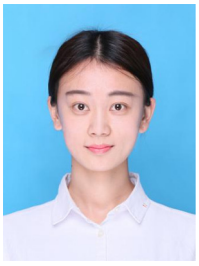

Ping Cheng received her B.S. in Light Chemical Engineering from the School of Zhejiang Sci-Tech University in 2016, and then entered Soochow University and Beijing Institute of Nanoenergy and Nanosystems, Chinese Academy of Sciences as a joint student. Now she is a Ph.D. candidate in the school of Institute of Functional Nano & Soft Materials (FUNSOM), Soochow University. Her research interests mainly focus on triboelectric nanogenerator for blue energy.

Hengyu Guo received his B. S. and Ph.D. degree in Applied Physics from Chongqing University, China. Now he is a postdoctoral fellow in Georgia institute of technology, Zhong Lin Wang' group. His current research interest is triboelectric nanogenerator based energy and sensor systems.

Zhen Wen received his B.S. degree in Materials Science and Engineering from China University of Mining and Technology (CUMT) in 2011 and Ph.D. degree in Materials Physics and Chemistry from Zhejiang University (ZJU) in 2016. During 2014–2016, he was supported by the program of China Scholarship Council (CSC) as a joint Ph.D. student in Georgia Institute of Technology (GT). He has joined in Institute of Functional Nano & Soft Materials (FUNSOM), Soochow University as an assistant professor since the end of 2016. His main research interests focus on triboelectric nanogenerator based energy harvesting and self-powered sensing system.

Chunlei Zhang received his B.S. degree in Material Science and Engineering from Nanjing University of Aeronautics and Astronautics University in 2016. Now, he is a postgraduate student in Beijing Institute of Nanoenergy and Nanosystems, Chinese Academy of Sciences, China. His current research interest is triboelectric nanogenerator based on energy storage and self-power system.

Xing Yin received his master degree from Southwestern Institute of Physics in 2013. Now, he is a Ph.D. Candidate in Beijing Institute of Nanoenergy and Nanosystems, Chinese Academy of Sciences. His current research is triboelectric nanogenerator based on energy storage and self-power system.

Xinyuan Li received her B.S. degree in chemistry from Minzu University of China. Now she is a postgraduate student in Beijing Institute of Nanoenergy and Nanosystems, Chinese Academy of Sciences, China. Her current research interest is relationship between triboelectric nanogenerator and energy storage devices for self-powered systems.

Di Liu received his B.S. degree in Material Science and Engineering from Nanjing University of Aeronautics and Astronautics. Now he is a Ph.D. candidate in Beijing Institute of Nanoenergy and Nanosystems, Chinese Academy of Sciences, China. His current research interest is triboelectric nanogenerator for energy harvesting and self-powered systems.

Dr. Song earned doctoral degree from ICCAS in 2009, and had studied in Max-Planck-Institute of Colloids and interfaces in Germany (2006–2009). Her research focuses on energy harvesting based on nanogenerators and solar cells, energy storage such as batteries and supercapacitors, and self-powered flexible electronics.

Xuhui Sun is a full professor at the Institute of Functional Nano & Soft Materials (FUNSOM) at Soochow University. He received his Ph.D. degree from the City University of Hong Kong in 2002. He performed postdoctoral research at the University of Western Ontario, Canada from 2003 to 2005 and at NASA Ames Research Center, USA from 2005 to 2007. He became a research scientist at NASA and adjunct assistant professor at Santa Clara University in 2007. His research interests include nanoelectronics, energy harvesting, nanosensors, and the development and application of synchrotron radiation techniques.

Dr. Jie Wang received her Ph.D. degree from Xi'an Jiaotong University in 2008. He is currently a professor at Beijing Institute of Nanoenergy and Nanosystems, Chinese Academy of Sciences. His current research interests focus on the energy materials, supercapacitors, nanogenerators and self-powered system.

Zhong Lin (ZL) Wang received his Ph.D. from Arizona State University in physics. He now is the Hightower Chair in Materials Science and Engineering, Regents' Professor, Engineering Distinguished Professor and Director, Center for Nanostructure Characterization, at Georgia Tech. Dr. Wang has made original and innovative contributions to the synthesis, discovery, characterization and understanding of fundamental physical properties of oxide nanobelts and nanowires, as well as applications of nanowires in energy sciences, electronics, optoelectronics and biological science. His discovery and breakthroughs in developing nanogenerators established the principle and technological road map for harvesting mechanical energy from environment and biological systems for powering a personal electronics. His research on self-powered nanosystems has inspired the worldwide effort in academia and industry for studying energy for micro-nano-systems, which is now a distinct disciplinary in energy research and future sensor networks. He coined and pioneered the field of piezotronics and piezo-phototronics by introducing piezoelectric potential gated charge transport process in fabricating new electronic and optoelectronic devices. Details can be found at: http://www.nanoscience.gatech.edu.